International Scholarly Research Network
ISRN Nanomaterials
Volume 2012, Article ID 890486, 4 pages
doi:10.5402/2012/890486

Research Article

Compression Experiments on γ'-Nanoparticles

Andreas Landefeld,[1] William M. Mook,[2,3] Joachim Rösler,[1] and Johann Michler[3]

[1] *Institut für Werkstoffe, Technische Universität Braunschweig, Langer Kamp 8, 38106 Braunschweig, Germany*
[2] *Center for Integrated Nanotechnologies, Los Alamos National Laboratory, Los Alamos, NM 87545, USA*
[3] *EMPA, Swiss Federal Laboratories for Materials Science and Technology, Laboratory for Mechanics of Materials and Nanostructures, Feuerwerkerstrasse 39, 3602 Thun, Switzerland*

Correspondence should be addressed to Andreas Landefeld, a.landefeld@tu-bs.de

Received 18 July 2012; Accepted 7 August 2012

Academic Editors: G. Dirras and F. Sansoz

The mechanical behavior of cubic γ'-nanoparticles is investigated in uniaxial compression. These nanoparticles are freestanding, single crystalline and have a well-defined crystallography related to the cubic geometry (cube faces correspond to the crystallographic {100}-planes). The true values of stress and strain were measured and evaluated. With a true strength of about 3000 MPa to 5000 MPa the nanoobjects reach a significant portion of the theoretical strength. Even after a true strain of about one, no signs of particle damage are observed.

1. Introduction

The utilization of microscopically small components in mechanically loaded microsystems requires (i) development of suitable fabrication processes on the micro- and nanoscale, see, for example, Hoxhold and Büttgenbach [1] and Landefeld and Rösler [2] as well as (ii) understanding of the mechanical behavior at reduced dimensions, see for example, [3–7]. One way to obtain freestanding metallic components on the nanoscale is to extract precipitates from alloys and deform them between microhammer and microanvil in the scanning electron microscope (SEM). This so-called nanoforging process was first described by Rösler et al. [8], using cube-shaped γ'-particles which were extracted from Ni-based superalloys. The purpose of this study is to investigate the flow behavior of these γ'-nanoparticles for the following reasons. Firstly, understanding the flow strength and the deformability is of crucial importance for control and optimization of the nanoforging process. Secondly, the strength of the nanoforged γ'-particles has to be known if they are to be used in mechanically loaded microdevices and the strength is also of interest with regard to the common destination of γ'-particles as hardening phase in Ni-base superalloys. Thirdly, there is fundamental interest in the mechanical behavior of metallic materials on the nanoscale as mentioned above and deformation experiments on γ'-particles are particularly attractive for the following reasons. Compared to micro- and nanopillars, see for example, [5, 9], the γ'-particles are freestanding, thus avoiding constraints by attachment to a substrate. Furthermore, the electrochemical extraction process as described in [10, 11] does not lead to surface damage and TEM investigations have confirmed that the particles are essentially defect-free [12]. Compared to deformation experiments on gold particles [3, 4], the benefit is that the stress field in the cube-shaped particles is more uniform on compression, so that stress gradients are less influential.

2. Results and Discussion

First of all Schloesser et al. [13] studied the deformation behavior of γ'-particles, extracted from Ni-base superalloys. However, the experimental setup used was optimized for the forging process rather than for precise measurement of the stress-strain response, thus limiting the accuracy of the results. Further research on compression of γ' was also done by Maaß et al. [14]. They compared the stress and displacement of as-extracted γ'-particles with particles irradiated by focused ion beam. In this study, the deformation

Table 1: Yield strength σ_y, critical resolved shear stress τ_s and normalized critical resolved shear stress $\tau_s/G_{[111][\bar{1}01]}$ for the conducted compression experiments.

Exp.	σ_y [MPa]	τ_s [MPa]	$\tau_s/G_{[111][\bar{1}01]}$
P1	3799	1550	0.025
P2	2954	1205	0.020
P3	4824	1968	0.032
P4	3691	1506	0.025
P5	4213	1719	0.028
P6	3378	1378	0.023

behavior of cube-shaped γ'-particles extracted from the superalloy CMSX-4 [15] was investigated using a Hysitron SEM-Picoindenter with a boron-doped-flat punch diamond tip and a Si wafer as substrate. To observe and document the deformation process at the same time, the indenter was placed in a Hitachi S-4800 SEM equipped with a cold field emission gun. The compression of the nanoparticles was conducted with a loading rate of 2 μN/s, followed by fast load release. Because of uneven surfaces and setting during contact, the stress-strain-response from 0 kN to 100 kN was back-extrapolated using the linear slope of the stress-strain-curve in the range from 100 kN to 150 kN. For compression testing, the assembly of Indenter and Si-substrate is tilted such that loading axis and direction of the electron beam are at an angle of 80°. Prior to each compression test, the height h_0 and cross-sectional area A_0 of each γ'-particle were measured (see Figures 1(a) and 1(b)). Care was taken to only select particles with nearly cubic shape (see Figures 1(a) and 1(b)). While testing, no significant plastic deformation of punch and substrate was observed or is soluble with a cold-field emission SEM. The true stress is plotted in Figure 2 versus the true strain for the conducted experiments. All curves are characterized by linear elastic behavior up to a yield strength of about 3000 to 5000 MPa (see Table 1). With Schmid-factor $S = 0.408$ for slip along $\{111\}\langle\bar{1}01\rangle$-type slip systems, a critical resolves shear stresses of about 1200 MPa to 2000 MPa at the onset of plastic deformation results (Table 1). Taking the elastic data from Yasuda et al. [16] for Ni_3 (Al, Ti) single crystals, the shear modulus $G_{[111][\bar{1}01]} = 61$ GPa is obtained for slip along a (111)-plane in $[\bar{1}01]$-direction after transformation of the stiffness tensor into the new coordinate system with the coordinate axes oriented parallel to $[\bar{1}01]$, [111], and $[\bar{1}2\bar{1}]$ [17]. Thus onset occurs when the critical resolved shear stress reaches about 2% to 3% of the shear modulus (Table 1), which is a significant portion of the theoretical strength. Once the yield strength is reached and plastic deformation sets in, the flow strength drops (see Video S1). Only after large deformations is the load high enough again (due to the increased cross-sectional area) for the load-controlled deformation process to become stable again. After some further load increase, the samples were unloaded and the elastic strain recovered (Figure 2). A similiar behavior is observed in Mook et al. [3] for facetted Au-particles.

Fundamentally, the stress-strain behavior is as reported in [13]. However, the more precise data obtained here show clearly that the material response up to the peak stress is merely elastic, whereas the data in [13] suggested prior plastic deformation. Once the peak stress, that is the yield point, is reached and plastic deformation sets in, the flow strength of the γ'-particle drops dramatically. Consequently, the particle collapses unstably during the load-controlled experiment, leading to a large strain burst (see Figure 2 and Video S1). Its deformation rate during this strain burst is far too high to monitor an image of the deforming particle in the SEM. The aspect ratio of the cross-section is similar before and after the strain burst. Please note that the view of the compressed particle in Figure 1(d) is slightly tilted because the particle was stripped at the edge of the Si-substrate after compression testing. Clearly visible on the particle surface are parallel slip lines (Figures 1(c) and 1(d)). In this study, the true values of stress and strain were determined. The engineering stresses are higher and almost in accordance with the main value of the yield stress measured by Maaß et al. [14] on γ'-particles.

From these findings, we deduce the following sequence of events during loading of the γ'-particles. Initially, the tested γ'-particles were without mobile defects and were most likely dislocation-free which is in accordance with the findings in [12], so that solely elastic behavior results up to a very high stress level. Once the yield point is reached on compression, the stresses are sufficiently high for dislocation nucleation from the particle surface to take place. As soon as the first dislocation is nucleated, it is driven through the entire crystal by the resolved shear stress, leaving a surface step behind. This step is facilitating the nucleation of the next dislocations, so that the dislocation nucleation rate is drastically increasing and an avalanche-like deformation process sets in. As the deformation process is continuing and the aspect ratio of the particle is decreasing, deformation of the particle can no longer be supported by slip on one (or a few) slip plane(s) for geometric reasons, so that more and more slip systems have to be activated, leading to strain hardening and the generation of back stresses. Furthermore, the true stress is decreasing due to an increasing cross-sectional area. Both factors counter dislocation nucleation so that the strain burst comes to an end after a certain amount of strain.

Qualitatively speaking, the observed deformation behavior is analogous to that of whiskers [18] and micropillars prepared by electrochemical etching [19], which is also the method used here to extract the γ'-particles from the superalloy. Salient features are a yield strength close to the theoretical strength, followed by plastic deformation at vastly reduced stress levels. Presumably, they are characteristic for initially dislocation- and defect-free specimens. In contrast, deformation experiments performed on micropillars produced by focused ion beam milling show different characteristics, namely, a multitude of smaller strain bursts starting at significantly lower stress levels and a steady increase of the flow strength to a plateau value (except for limited stress drops associated with the strain bursts). As mentioned previously [14, 19], this difference in the stress-strain response is likely a consequence of FIB-induced surface defects. It stands to reason that these defects facilitate

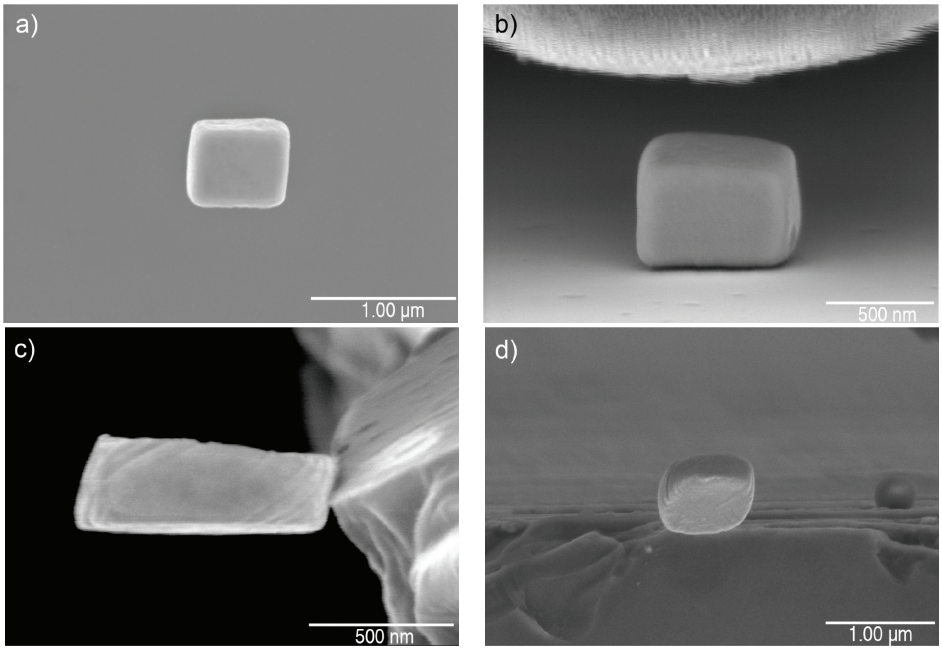

Figure 1: SEM images of the particle P6. Top view (a, c) and side view (b, d) before (a, b) and after (c, d) the compression test.

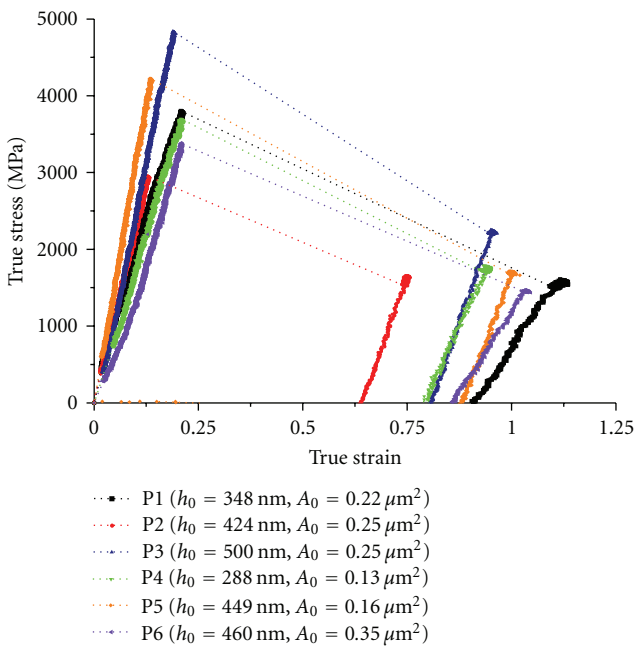

Figure 2: True Stress-True Strain Curves of γ'-Particles.

dislocation nucleation, thus leading to onset of plastic deformation at reduced stress levels and a sequence of strain bursts as different dislocation sources are activated at different stress levels.

Finally, we come back to the issue of nanoforging. Firstly, it is noticed that the true compressive stress after the strain burst has stopped is similar for all investigated particles. The true stress is on the order of 2000 MPa. Even though it is difficult to determine the exact flow strength of the deformed γ'-particles from that number because their pancake-like shapes lead to significant friction forces, their flow strength is apparently still very high. Secondly, a striking result is the excellent deformability of the γ'-particles at ambient temperature despite of their high flow strength. Even after a true strain of about one, no signs of particle damage are observed. This combination of strength and deformability is unmatched in the macroscopic world. The reason is that the γ'-raw stock used for the forging process is defect-free because of its dimension on the nanoscale while defects such as pores or hard inclusions cannot be entirely avoided in the macroscopic world. Thus, the data obtained here demonstrate a distinct advantage in terms of strength and deformability when the forging technology is extended from the macroscopic to the microscopic world, which makes nanoforging particularly attractive.

References

[1] B. Hoxhold and S. Büttgenbach, "Easily manageable, electrothermally actuated silicon micro gripper," *Microsystem Technologies*, vol. 16, no. 8-9, pp. 1609–1617, 2010.

[2] A. Landefeld and J. Rösler, "Fabrication of metallic nanocomponents by forging of Ni_3Al-nanoparticles," in *MRS Proceedings*, vol. 1412, 2012.

[3] W. M. Mook, C. Niederberger, M. Bechelany, L. Philippe, and J. Michler, "Compression of freestanding gold nanostructures: from stochastic yield to predictable flow," *Nanotechnology*, vol. 21, no. 5, 2010.

[4] D. Mordehai, S. W. Lee, B. Backes, D. J. Srolovitz, W. D. Nix, and E. Rabkin, "Size effect in compression of single-crystal

gold microparticles," *Acta Materialia*, vol. 59, no. 13, pp. 5202–5215, 2011.

[5] J. R. Greer, W. C. Oliver, and W. D. Nix, "Size dependence of mechanical properties of gold at the micron scale in the absence of strain gradients," *Acta Materialia*, vol. 53, pp. 1821–1830, 2005.

[6] D. Kiener, W. Grosinger, G. Dehm, and R. Pippan, "A further step towards an understanding of size-dependent crystal plasticity: in situ tension experiments of miniaturized single-crystal copper samples," *Acta Materialia*, vol. 56, no. 3, pp. 580–592, 2008.

[7] W. W. Gerberich, W. M. Mook, C. R. Perrey et al., "Superhard silicon nanospheres," *Journal of the Mechanics and Physics of Solids*, vol. 51, no. 6, pp. 979–992, 2003.

[8] J. Rösler, D. Mukherji, K. Schock, and S. Kleindiek, "Forging of metallic nano-objects for the fabrication of submicron-size components," *Nanotechnology*, vol. 18, no. 12, 2007.

[9] S. W. Lee, S. M. Han, and W. D. Nix, "Uniaxial compression of fcc Au nanopillars on an MgO substrate: the effects of prestraining and annealing," *Acta Materialia*, vol. 57, pp. 4404–4415, 2009.

[10] J. Rösler, O. Näht, S. Jäger, F. Schmitz, and D. Mukherji, "Fabrication of nanoporous Ni-based superalloy membranes," *Acta Materialia*, vol. 53, pp. 1397–1406, 2005.

[11] D. Mukherji, G. Pigozzi, F. Schmitz, O. Näth, J. Rösler, and G. Kostorz, "Nano-structured materials produced from simple metallic alloys by phase separation," *Nanotechnology*, vol. 16, pp. 2176–2187, 2005.

[12] D. Mukherji, R. Müller, and R. Gilles, "Nanocrystalline Ni_3Al-type intermetallic phase powder from Ni-base superalloys," *Nanotechnology*, vol. 15, no. 5, pp. 648–657, 2004.

[13] J. Schloesser, J. Rösler, and D. Mukherji, "Deformation behaviour of freestanding single-crystalline Ni_3Al-based nanoparticles," *International Journal of Materials Research*, vol. 102, no. 5, pp. 532–537, 2011.

[14] R. Maaß, L. Meza, B. Gan, S. Tin, and J. Greer, "Ultrahigh strength of dislocation-free Ni_3Al Nanocubes," *Small*, vol. 8, no. 12, pp. 1869–1875, 2012.

[15] K. Harris, G. L. Erickson, S. L. Sikkenga, W. D. Brentnall, I. M. Aurrecoechea, and K. G. Kubarych, "Development of the rhenium containing superalloys CMSX-4 and CM186 LC for single crystal blade and directionally solidified vane applications in advanced turbine engines," in *Proceedings of the 7th International Symposium on Superalloy*, K. A. Green et al., Ed., pp. 297–306, 1992.

[16] H. Yasuda, T. Takasugi, and M. Koiwa, "Elasticity of Ni-based L12-type intermetallic compounds," *Acta Metallurgica et Materialia*, vol. 40, pp. 381–387, 1992.

[17] U. Bayerlein, *Zur Ermittlung der Textur- und Gefügeabhängigkeit der elastischen Eigenschaften sowie der Einkristallkonstanten von Superlegierungen bei höheren Temperaturen*, VDI, 1991.

[18] S. S. Brenner, "Tensile strength of whiskers," *Journal of Applied Physics*, vol. 27, no. 12, pp. 1484–1491, 1956.

[19] S. Shim, H. Bei, M. K. Miller, G. M. Pharr, and E. P. George, "Effects of focused ion beam milling on the compressive behavior of directionally solidified micropillars and the nanoindentation response of an electropolished surface," *Acta Materialia*, vol. 57, pp. 503–510, 2009.